Dressed-State Amplification by a Single Superconducting Qubit

G. Oelsner,[1] P. Macha,[1] O. V. Astafiev,[2] E. Il'ichev,[1] M. Grajcar,[3] U. Hübner,[1] B. I. Ivanov,[1] P. Neilinger,[3] and H.-G. Meyer[1]

[1]*Institute of Photonic Technology, P.O. Box 100239, D-07702 Jena, Germany*
[2]*NEC Smart Energy Research Laboratories, Tsukuba, Ibaraki 305-8501, Japan*
[3]*Department of Experimental Physics, Comenius University, SK-84248 Bratislava, Slovakia*

(Received 31 July 2012; published 30 January 2013)

We demonstrate amplification of a microwave signal by a strongly driven two-level system in a coplanar waveguide resonator. The effect, similar to the dressed-state lasing known from quantum optics, is observed with a single quantum system formed by a persistent current (flux) qubit. The transmission through the resonator is enhanced when the Rabi frequency of the driven qubit is tuned into resonance with one of the resonator modes. Amplification as well as linewidth narrowing of a weak probe signal has been observed. The stimulated emission in the resonator has been studied by measuring the emission spectrum. We analyzed our system and found an excellent agreement between the experimental results and the theoretical predictions obtained in the dressed-state model.

DOI: 10.1103/PhysRevLett.110.053602 PACS numbers: 42.50.Pq

A coherently strongly driven two-level system can efficiently be described by dressing of the energy levels. Dressed states are attracting renewed interest in different fields of physics, connected with quantum information processing. Recently it was shown that microwave dressed states can be used to extend coherence times by 2 orders of magnitude [1]. On the other hand, the concept of using similar coherently strongly driven two-level systems for inversionless amplification of a probe field was pioneered several decades ago [2–4]. The coupling between the driving field and the two-level quantum system is characterized by the Rabi frequency. Two resonances occur at the Rabi sidebands with the frequencies [5]

$$\omega_s = \omega_d \pm \Omega_R, \tag{1}$$

where $\Omega_R = \sqrt{\Omega_{R0}^2 + \delta^2}$ is the generalized Rabi frequency with a detuning $\delta = \omega_d - \omega_q$ between driving field frequency ω_d and qubit transition frequency ω_q. Ω_{R0} is the on-resonance Rabi frequency. The analysis of such systems shows that there is an absorption of the probe field at one of the Rabi sidebands ($\omega_p = \omega_d + \Omega_R$) and a gain at the other one ($\omega_p = \omega_d - \Omega_R$). Indeed, the amplification (damping) was realized experimentally by Wu *et al.* [6], and lasing was demonstrated by Khitrova *et al.* [7]. However, an interaction directly at the Rabi frequency is not visible for such systems (at least not in first order), because the dipole moment does not give transition elements between the split states.

The active medium of conventional lasers and amplifiers consists of many quantum systems, which are usually molecules and atoms. Due to the tiny size of these objects, they are weakly coupled to the cavity. Nevertheless, the strong coupling regime has been achieved and a single atom laser, with vanishing pumping threshold, has been convincingly demonstrated [8]. By using superconducting qubits as artificial atoms this regime can be achieved easily. As a consequence, lasing action with a single Josephson-junction charge qubit has been realized [9].

Characteristic frequencies of superconducting qubits belong to the microwave frequency range. Recent activities, motivated by quantum limited measurements and the implementation of quantum information processing devices, require extremely low-noise microwave amplifiers. Such amplifiers are usually based on the nonlinearity of superconducting weak links [10,11]. Recently, the squeezing of quantum noise and its measurement below the standard quantum limit was demonstrated [12]. These experiments motivated the development of a new generation of parametric amplifiers based on "classical" Josephson junction structures [13,14]. However, quantized energy levels of superconducting qubits can also be used for these purposes. For instance, the stimulated emission by a superconducting qubit was successfully employed for the amplification of a microwave signal passing through a transmission line [15].

In this Letter, we show that the concept of dressed-state lasers [5,16] can be used for the amplification of a microwave signal. We demonstrate experimentally a proof of principle of a dressed-state amplifier with a single two-level system and provide a full theoretical analysis. The present realization exploits the direct transition at the Rabi frequency Ω_R [17,18] rather than the sideband transitions ω_s. The Rabi frequency is tuned into resonance with the oscillator, providing a qubit-resonator energy exchange. A direct interaction at the Rabi frequency becomes possible only for a tuneable two-level system and was demonstrated in a NMR experiment [19].

In order to show dressed-state amplification we have chosen a flux (or persistent-current qubit) as an artificial

atom, coupled to a superconducting coplanar waveguide resonator. The niobium (Nb) resonator was fabricated by e-beam lithography and dry etching of a 200-nm-thick Nb film deposited on a silicon substrate. The length of the resonator's central conductor is $L \simeq 23$ mm, which results in a resonance frequency of $\omega_r/2\pi \approx 2.5$ GHz for the fundamental half-wavelength mode. The width of the central conductor is 50 μm, and the gap between the central conductor and the ground plane is 30 μm resulting in a wave impedance of about 50 Ω. In the middle of the resonator the central conductor is tapered to a width of 1 μm for a length of 30 μm with 9 μm gap (see Fig. 1), which provides better qubit-resonator coupling and a small impedance mismatch to detune the harmonics of the resonator. We achieved a separation of about 25 linewidths between the multiple of the fundamental mode frequency $3\omega_r$ and third harmonic ω_{3H}. At milliKelvin temperatures the resonator quality factor is measured to be $Q \simeq 4 \times 10^4$.

The aluminum flux qubit was fabricated in the central part of the resonator by conventional shadow evaporation technique. The qubit loop size (12×5 μm^2) is interrupted by three Josephson junctions. Two of them have a nominal size of (550×120 nm^2), while the third is about 25% smaller. Two cryoperm shields and one superconducting shield are used to minimize the influence of the external magnetic fields. The sample was thermally anchored to the mixing chamber of a dilution refrigerator, providing a base temperature of about 10 mK.

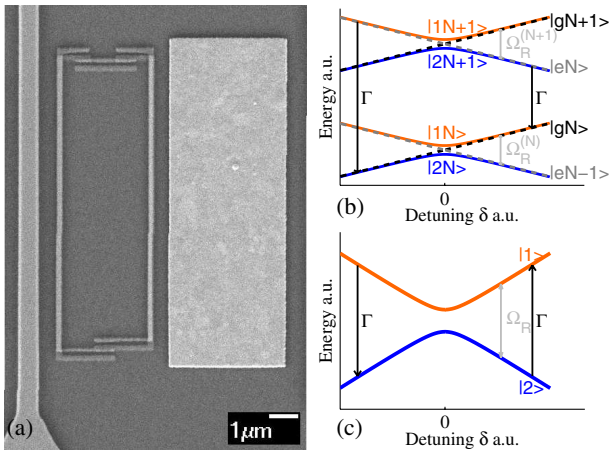

FIG. 1 (color online). (a) Electron micrograph of the central part of the resonator: the central line of the resonator (left), qubit (middle), and the gold film resistor (right). (b) Sketch of the dressed system manifolds N and $N+1$. The dashed lines correspond to the uncoupled states. The qubit relaxation with rate Γ is sketched for the uncoupled states. When coupled the levels will split depending on the photon state N. The level spacing between those split states is given by the generalized Rabi frequency Eq. (4). (c) After tracing over the photon number N an effective two-level system, denoted with states $|1\rangle$ and $|2\rangle$ is obtained. Both the sign and strength of the relaxation (excitation) in this system depend on the detuning [see Eq. (7)].

The parameters of the qubit, the persistent current $I_p = 12$ nA, and the minimum transition frequency (gap) $\Delta/2\pi = 3.7$ GHz were determined from the transmission of the resonator measured as a function of the qubit transition frequency. As the gap of the qubit is higher than the frequency of the fundamental mode, we observe a dispersive shift of the resonator's fundamental frequency. The energy gap and persistent current of the qubit were separately determined from this dispersive shift [20] and from resonant interaction [21,22] combined with the positions of the anticrossings [23,24]. Similar to Ref. [25] both sets of data are consistent.

For the flux qubit an unusually low persistent current was chosen for emission stability and efficiency. We decreased the critical current of the Josephson junctions and increased the energy difference of the two-level system to make it more immune against flux fluctuation [26]. Although the qubit became more sensitive to charge fluctuation, we did not observe any significant charge noise effects. In addition, the relaxation time was intentionally decreased by a gold resistor placed next to the qubit loop (see Fig. 1).

Throughout this letter the frequency of the driving signal ω_d is fixed at the frequency of the third harmonic of the resonator $\omega_d = \omega_{3H}$. Therefore, the photon field created in the third harmonic (driving mode) is driving the qubit, since the odd harmonics of the resonator provide optimal coupling of the field to the qubit.

In the first set of experiments the transmission of a weak coherent probe signal, populating the resonator with an average photon number less than one, was measured at frequencies ω_p close to the fundamental mode frequency ω_r. Similar to the proposal in Ref. [27], we use the dressing of the qubit states introduced by the driving signal to create interaction with the resonator's fundamental mode. The dependence of the transmission on the qubit transition frequency is shown in Fig. 2.

The two dark areas correspond to amplification. This amplification is observed when the generalized Rabi frequency Ω_R is tuned to the frequency of the fundamental mode ω_r. The Rabi frequency depends on the driving strength at ω_d and the transition frequency of the qubit $\omega_q = \sqrt{\Delta^2 + \epsilon^2}$ (see below). Here, $\hbar\epsilon = \Phi_0 I_p(2\Phi_x/\Phi_0 - 1)$ is the energy bias of the qubit and Φ_0 is the magnetic flux quantum. Φ_x is the external flux in the qubit loop.

Quantitatively, the amplitudes of the resonance curves at these points are increased by 10% and show linewidth narrowing, see inset in Fig. 2. Thus, the resonator loss rate is reduced by about 10%. For quantitative analysis, we consider the Hamiltonian of a qubit interacting with the photon fields of two resonator modes, using an approach similar to Refs. [17,18]. However, we use a quantized description of the fields in the resonator at fundamental mode ω_r and driving mode ω_d. The latter is described by

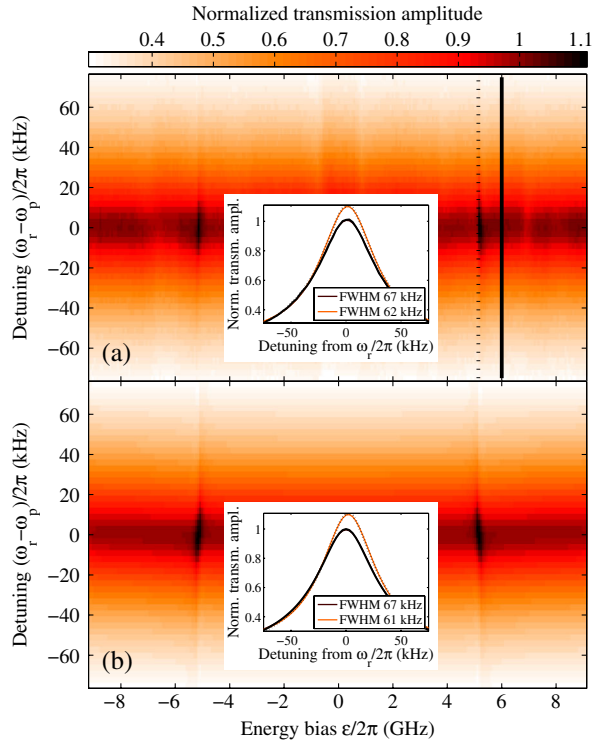

FIG. 2 (color online). (a) Normalized transmission amplitude of the probe signal as a function of $(\omega_p - \omega_r)/2\pi$ and qubit energy bias $\epsilon/2\pi$. The inset shows two cuts of this figure, visible as the Lorentzian shaped transmission vs. $(\omega_p - \omega_r)/2\pi$ in the amplification point (corresponding to $\delta = 1.4$ GHz, dashed line) and out of the Rabi resonance (solid line). The experiments were done in the presence of a strong driving field, corresponding to 8 pW at the input of the resonator, applied at the third harmonic frequency. The driving strength defines the on-resonance Rabi frequency. (b) Numerical simulations by making use of Eq. (6) in a four photon space. The probing power is assumed to be weak creating a coherent state with a mean photon number less than one in the fundamental mode.

the creation and annihilation operators $b^\dagger$ and b, and the coupling between this field and the qubit is characterized by the energy $\hbar g_d$. The qubit is represented by the Hamiltonian $H_q = \frac{\hbar\omega_q}{2}\sigma_z$ in the basis of the ground and excited states $|g\rangle$ and $|e\rangle$. $\sigma_{x,y,z}$ are the Pauli matrices. By neglecting the diagonal coupling term, proportional to σ_z, as well as the nonresonant terms ($b^\dagger\sigma_+$ and $b\sigma_-$, where $\sigma_\pm = (\sigma_x \pm i\sigma_y)/2$), we arrive at the Jaynes-Cummings Hamiltonian

$$H_d = \hbar\omega_d\left(b^\dagger b + \frac{1}{2}\right) + \hbar\frac{\omega_q}{2}\sigma_z + \hbar g_d\frac{\Delta}{\omega_q}(b^\dagger\sigma_- + b\sigma_+). \tag{2}$$

By diagonalization the Hamiltonian is transformed to the dressed-state basis. This yields a ladder

$$H_d = \hbar\omega_d\hat{n} + \frac{\hbar}{2}\hat{\Omega}_R, \tag{3}$$

where we have introduced the number operator $\hat{n} = \sum_N N(|1N\rangle\langle 1N| + |2N\rangle\langle 2N|)$ and the Rabi operator $\hat{\Omega}_R = \sum_N \Omega_R^{(N)}(|1N\rangle\langle 1N| - |2N\rangle\langle 2N|)$. The dressed states $|1N\rangle$ and $|2N\rangle$ are found by a standard transformation [28]. We use the modified generalized Rabi frequency as

$$\Omega_R^{(N)} = \sqrt{\delta^2 + 4g_d^2 N\Delta^2/\omega_q^2}, \tag{4}$$

where $\delta = \omega_d - \omega_q$ is the detuning between the qubit frequency and the driving signal frequency. For large N and small deviations from the average photon number $\langle N\rangle$ of the driving cavity field, $\Omega_R^{(N)}$ can be substituted by the constant value $\Omega_R = \Omega_R^{(\langle N\rangle)}$. In the dressed-state basis the interaction between the dressed-state system and the resonator's fundamental mode is described by the Hamiltonian

$$H = H_d + \hbar\omega_r a^\dagger a + \hbar g_e\left(\frac{\Omega_{R0}}{\Omega_R}\sigma_x + \frac{\delta}{\Omega_R}\sigma_z\right)(a^\dagger + a) + H_p. \tag{5}$$

Here, the on-resonance Rabi frequency is defined as $\Omega_{R0} = 2g_d\Delta\sqrt{\langle N\rangle}/\omega_q$. The fundamental mode of the resonator is expressed by the product of the creation and annihilation operators $a^\dagger$ and a, g_e is the effective coupling constant of that mode to the qubit and the probing field is described by $H_p = \hbar\Omega_p\cos\omega_p t(a^\dagger + a)$. Note that the Hamiltonian in Eq. (5) reflects the dynamics at the Rabi frequency and the transitions between the dressed states from different manifold N are neglected.

The dynamics of this Rabi lasing system is essentially dissipative. The effects of dissipation can be accounted for by the Liouville equation for the density matrix of the system, including the relevant damping terms, which are assumed to be of Markovian form. The corresponding damping (Lindblad) terms are found for relaxation with rate Γ, decoherence with rate Γ_φ of the qubit and the photon decay of the resonator with rate κ.

The Liouville equation for the density matrix of the system can be written in the usual form

$$-\frac{i}{\hbar}[H^R, \rho] + L^R(\rho) + L_r(\rho) = 0 \tag{6}$$

for the reduced elements of the density matrix ρ. The Hamiltonian H^R and the damping terms, L^R from the qubit and L_r for the resonator, are written in the rotating dressed-state basis. Because the operators $a^\dagger$ and a are the same in both bases, the photon decay of the resonator's fundamental mode is not changed after this transformation. Nevertheless, the population of the dressed states itself is modified by the relaxation rates of the qubit [17]. By omitting the oscillating terms in the rotating frame, the qubit's dissipation in the dressed basis reads

$$L_{11}^R = \frac{\Gamma\delta_q}{2\Omega_R}(\rho_{11}+\rho_{22}) - \left[\frac{\Gamma\delta^2}{2\Omega_R^2} + \frac{\Gamma_\varphi\Omega_{R0}^2}{2\Omega_R^2}\right](\rho_{11}-\rho_{22})$$
$$L_{22}^R = -L_{11}^R, \tag{7}$$

$$L_{12}^R = \left[-\Gamma_\varphi + \frac{\Omega_{R0}^2}{2\Omega_R^2}(\Gamma_\varphi - \Gamma)\right]\rho_{12}$$
$$L_{21}^R = \left[-\Gamma_\varphi + \frac{\Omega_{R0}^2}{2\Omega_R^2}(\Gamma_\varphi - \Gamma)\right]\rho_{21}. \tag{8}$$

Here, $L_{jk}^R = \mathrm{tr}^{(N)}\langle jN|L_q|kN\rangle$; $j,k \in [1,2]$ are the reduced elements of the Lindblad operator for the dressed-state system, which yield from the Markovian Lindblad operator L_q in the qubit's eigenbasis. We introduced the reduced elements of the density matrix $\rho_{jk} = \mathrm{tr}^{(N)}\langle jN|\rho|kN\rangle$; $j,k \in [1,2]$ similarly. Because the states of this effective two-level system are formed by a superposition of qubit ground and excited state, the rate of relaxation depends on the weight of both states in this superposition. This is illustrated in Figs. 1(b) and 1(c). The relaxation is defined by the detuning. Moreover, for positive detuning δ the relaxation of the qubit forces the effective two-level system to the higher energetic state. Therefore, in the frame of the dressed-state model, a population inversion of the energy levels is created. For small detuning the decoherence rate equalizes the population of the two reduced dressed levels. The decoherence rate of the dressed states Eq. (8) is increased compared to that of the qubit. For large detuning, when $\Omega_{R0} \ll \Omega_R$ and $\delta/\Omega_R \approx 1$ the dissipative terms of the qubit are retrieved.

In order to find the quasi-steady-state density matrix we solved Eq. (6) numerically. We limited the photon space of the fundamental mode to a size of four, since we considered weak probing but expect an increasing photon number due to the amplification. The transmission of the resonator is then given by the expectation value of the annihilation operator $\langle a\rangle$ [24]. Theoretically and experimentally obtained transmission data are in good agreement (Fig. 2). We observe the amplification of the weak probe signal and the linewidth narrowing; see Fig. 2. By optimizing the parameters of the simulation we arrived at the values $g/2\pi \approx 0.8$ MHz, $\Gamma/2\pi \approx 80$ MHz, and $\gamma_\varphi \ll \Gamma$. The pure dephasing γ_φ is negligible relative to the relaxation rate, which was intentionally enhanced by the gold film resistor.

The power dependence of the amplification point (Fig. 3) has been described as well. The dotted line in Fig. 3(a) follows from the resonance condition $\Omega_R = \omega_p$. Consistence between theory and experiment was also found in this case. The optimum of the amplification process results from the dependence of the effective excitation rates and the coupling constant on the detuning δ, since a monotonic dependence of the qubit excitation rate

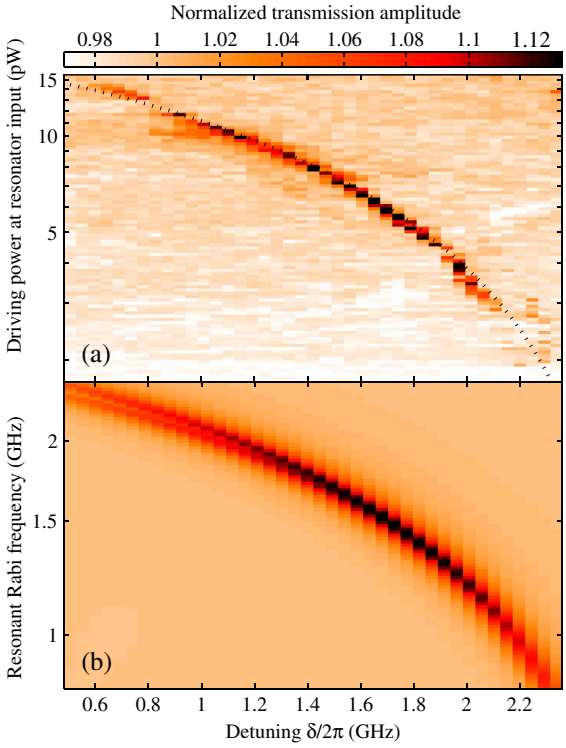

FIG. 3 (color online). (a) Normalized transmission amplitude as a function of the detuning δ (between the strong driving ω_d and the qubit transition frequency ω_q) and the driving power. The dashed line is calculated according to Eq. (4) and used to map the on-resonance Rabi frequency $\Omega_R^{\langle N\rangle}(\delta = 0)$ to the driving power. (b) Numerical simulations of the experimental results shown in (a) by use of Eq. (6).

($\Gamma \propto \delta/\Omega_R$) is compensated by the decreasing of the effective coupling ($g_e \propto \Omega_{R0}/\Omega_R$).

In a second set of experiments we removed the probing field and measured the emission of the resonator at its fundamental mode with optimum amplification parameters. The results are shown in Fig. 4. A strong increase of the emission in the presence of strong driving (open circles) was clearly observed, compared to the thermal response of the resonator (dots). Standard fitting of the data by Lorentzian curves demonstrates a linewidth narrowing. In general, this could indicate laser action in the system, but this issue requires further study.

In conclusion, we designed a superconducting resonator-qubit system and demonstrated experimentally the main features of dressed-state amplification of a probe field by a strongly driven qubit directly at the Rabi frequency. Linewidth narrowing for the transmission of the weak probe field was observed. Furthermore, free emission provided by the strong driving was detected. Numerical simulations performed in the frame of the dressed-state model and the experimental results are completely consistent. We believe that optimizations in the design could lead to the realization of new types of quantum microwave amplifiers and sources.

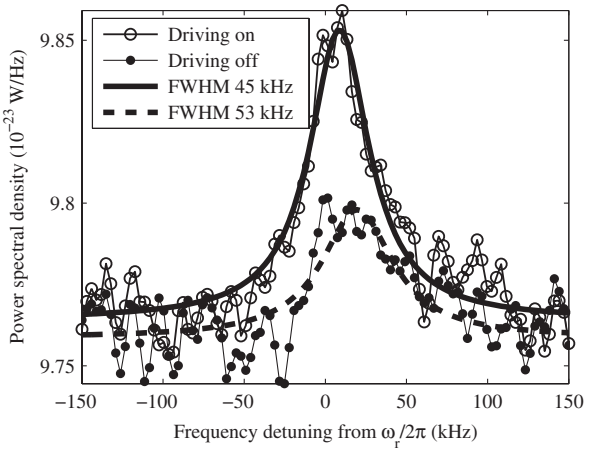

FIG. 4. Spectral emission from the resonator. The solid lines correspond to the best Lorentzian fits of the measured data and are used to reconstruct the linewidths. The power spectral density measured without driving field (dots) corresponds to the thermal occupation of the resonator at an effective temperature of 30 mK. The cold amplifier adds a background corresponding to a noise temperature of 7 K. If the lasing process is turned on by driving the resonator's third harmonic we observe a clear increase of the emission and a lower linewidth (open circles).

The research leading to these results has received funding from the European Community's Seventh Framework Programme (FP7/2007-2013) under Grant No. 270843 (iQIT). The authors gratefully acknowledge the financial support of the EU through the project SOLID and ERDF OP R&D, Project CE QUTE & metaQUTE. M. G. and P. N. were supported by the Slovak Research and Development Agency under Contracts No. APVV-0432-07, No. APVV-0515-10, and No. LPP-0159-09. G. O. thanks Ya. S. Greenberg and S. N. Shevchenko for helpful discussions.

[1] N. Timoney, I. Baumgart, M. Johanning, A. F. Varn, M. B. Plenio, A. Retzker, and Ch. Wunderlich, Nature (London) **476**, 185 (2011).
[2] S. G. Rautian and I. I. Sobel'man, Zh. Eksp. Teor. Fiz. **41**, 456 (1961) [Sov. Phys. JETP **14**, 328 (1962)].
[3] B. R. Mollow, Phys. Rev. A **5**, 2217 (1972).
[4] S. Haroche and F. Hartmann, Phys. Rev. A **6**, 1280 (1972).
[5] For review see J. Mompart and R. Corbalán, J. Opt. B **2**, R7 (2000).
[6] F. Y. Wu, S. Ezekiel, M. Ducloy, and B. R. Mollow, Phys. Rev. Lett. **38**, 1077 (1977).
[7] G. Khitrova, J. F. Valley, and H. M. Gibbs, Phys. Rev. Lett. **60**, 1126 (1988).
[8] J. McKeever, A. Boca, A. D. Boozer, J. R. Buck, and H. J. Kimble, Nature (London) **425**, 268 (2003).
[9] O. V. Astafiev, K. Inomata, A. O. Niskanen, T. Yamamoto, Yu. A. Pashkin, Y. Nakamura, and J. S. Tsai, Nature (London) **449**, 588 (2007).
[10] M. A. Castellanos-Beltran, K. D. Irwin, G. C. Hilton, L. R. Vale, and K. W. Lehnert, Nat. Phys. **4**, 929 (2008).
[11] T. Yamamoto, K. Inomata, M. Watanabe, K. Matsuba, T. Miyazaki, W. D. Oliver, Y. Nakamura, and J. S. Tsai, Appl. Phys. Lett. **93**, 042510 (2008).
[12] F. Mallet, M. A. Castellanos-Beltran, H. S. Ku, S. Glancy, E. Knill, K. D. Irwin, G. C. Hilton, L. R. Vale, and K. W. Lehnert, Phys. Rev. Lett. **106**, 220502 (2011).
[13] N. Bergeal, F. Schackhert, M. Metcalfe, R. Vijay, V. E. Manucharyan, L. Frunzio, D. E. Prober, R. J. Schoelkopf, S. M. Girvin, and M. H. Devoreti, Nature (London) **465**, 64 (2010).
[14] M. Hatridge, R. Vijay, D. H. Slichter, J. Clarke, and I. Siddiqi, Phys. Rev. B **83**, 134501 (2011).
[15] O. V. Astafiev, A. A. Abdumalikov, Jr., A. M. Zagoskin, Yu. A. Pashkin, Y. Nakamura, and J. S. Tsai, Phys. Rev. Lett. **104**, 183603 (2010).
[16] G. S. Agarwal, Phys. Rev. A **42**, 686 (1990).
[17] Ya. S. Greenberg, Phys. Rev. B **76**, 104520 (2007).
[18] J. Hauss, A. Fedorov, C. Hutter, A. Shnirman, and G. Schön, Phys. Rev. Lett. **100**, 037003 (2008).
[19] A. E. Mefed and V. A. Atsarkin, Pis'ma Zh. Eksp. Teor. Fiz., **25**, 233 (1977) [JETP Lett. **25**, 215 (1977)].
[20] E. Il'ichev, N. Oukhanski, Th. Wagner, H.-G. Meyer, A. Yu. Smirnov, M. Grajcar, A. Izmalkov, D. Born, W. Krech, and A. Zagoskin, Low Temp. Phys. **30**, 620 (2004).
[21] D. Born, V. I. Shnyrkov, W. Krech, Th. Wagner, E. Il'ichev, M. Grajcar, U. Hübner, and H.-G. Meyer, Phys. Rev. B **70**, 180501 (2004).
[22] A. Wallraff, D. I. Schuster, A. Blais, L. Frunzio, R.-S. Huang, J. Majer, S. Kumar, S. M. Girvin, and R. J. Schoelkopf, Nature (London) **431**, 162 (2004).
[23] G. Oelsner, S. H. W. van der Ploeg, P. Macha, U. Hübner, D. Born, S. Anders, E. Il'ichev, H.-G. Meyer, M. Grajcar, S. Wünsch, M. Siegel, A. N. Omelyanchouk, and O. Astafiev, Phys. Rev. B **81**, 172505 (2010).
[24] A. N. Omelyanchouk, S. N. Shevchenko, Ya. S. Greenberg, O. Astafiev, and E. Il'ichev, Low Temp. Phys. **36**, 893 (2010).
[25] A. Izmalkov, S. H. W. van der Ploeg, S. N. Shevchenko, M. Grajcar, E. Il'ichev, U. Hübner, A. N. Omelyanchouk, and H.-G. Meyer, Phys. Rev. Lett. **101**, 017003 (2008).
[26] J. Q. You, Xuedong Hu, S. Ashhab, and F. Nori, Phys. Rev. B **75**, 140515(R) (2007).
[27] Y. X. Liu, C. P. Sun, and F. Nori, Phys. Rev. A **74**, 052321 (2006).
[28] C. Cohen-Tannoudji, J. Dupont-Rock, and G. Grynberg, *Atom-Photon Interactions. Basic Principles and Applications* (John Wiley, New York, 1998).